AGU PUBLICATIONS

Geophysical Research Letters

RESEARCH LETTER
10.1002/2016GL068689

Special Section:
First results from NASA's Magnetospheric Multiscale (MMS) Mission

Observations of energetic particle escape at the magnetopause: Early results from the MMS Energetic Ion Spectrometer (EIS)

I. J. Cohen[1], B. H. Mauk[1], B. J. Anderson[1], J. H. Westlake[1], D. G. Sibeck[2], B. L. Giles[2], C. J. Pollock[2,3], D. L. Turner[4], J. F. Fennell[4], J. B. Blake[4], J. H. Clemmons[4], A. N. Jaynes[5], D. N. Baker[5], J. V. Craft[5], H. E. Spence[6], J. T. Niehof[6], G. D. Reeves[7], R. B. Torbert[6], C. T. Russell[8], R. J. Strangeway[8], W. Magnes[9], K. J. Trattner[5], S. A. Fuselier[10,11], and J. L. Burch[10]

[1]The Johns Hopkins University Applied Physics Laboratory, Laurel, Maryland, USA, [2]NASA Goddard Space Flight Center, Greenbelt, Maryland, USA, [3]Now at Denali Scientific, Healy, Alaska, USA, [4]Aerospace Corporation, El Segundo, California, USA, [5]LASP, University of Colorado Boulder, Boulder, Colorado, USA, [6]Space Science Center, University of New Hampshire, Durham, New Hampshire, USA, [7]Los Alamos National Laboratory, Los Alamos, New Mexico, USA, [8]University of California, Los Angeles, California, USA, [9]Space Research Institute, Austrian Academy of Sciences, Graz, Austria, [10]Southwest Research Institute, San Antonio, Texas, USA, [11]Department of Physics and Astronomy, University of Texas at San Antonio, San Antonio, Texas, USA

Key Points:
- MMS/EIS observations afford new opportunities to study energetic (greater than tens of keV) particle interactions and escape across the magnetopause
- Early MMS/EIS observations reveal a new signature requiring boundary-normal magnetic fields at the dayside dusk magnetopause
- MMS/EIS observes simultaneous streaming of both electrons and light ion species, previously unexpected due to magnetic drift-shadowing

Supporting Information:
- Supporting Information S1
- Figure S1

Correspondence to:
I. J. Cohen,
ian.cohen@jhuapl.edu

Citation:
Cohen, I. J., et al. (2016), Observations of energetic particle escape at the magnetopause: Early results from the MMS Energetic Ion Spectrometer (EIS), *Geophys. Res. Lett.*, *43*, 5960–5968, doi:10.1002/2016GL068689.

Received 15 MAR 2016
Accepted 17 MAY 2016
Accepted article online 23 MAY 2016
Published online 20 JUN 2016

Abstract Energetic (greater than tens of keV) magnetospheric particle escape into the magnetosheath occurs commonly, irrespective of conditions that engender reconnection and boundary-normal magnetic fields. A signature observed by the Magnetospheric Multiscale (MMS) mission, simultaneous monohemispheric streaming of multiple species (electrons, H^+, He^{n+}), is reported here as unexpectedly common in the dayside, dusk quadrant of the magnetosheath even though that region is thought to be drift-shadowed from energetic electrons. This signature is sometimes part of a pitch angle distribution evolving from symmetric in the magnetosphere, to asymmetric approaching the magnetopause, to monohemispheric streaming in the magnetosheath. While monohemispheric streaming in the magnetosheath may be possible without a boundary-normal magnetic field, the additional pitch angle depletion, particularly of electrons, on the magnetospheric side requires one. Observations of this signature in the dayside dusk sector imply that the static picture of magnetospheric drift-shadowing is inappropriate for energetic particle dynamics in the outer magnetosphere.

1. Introduction

Magnetospheric energetic particles (greater than tens of keV) are often present in the magnetosheath [e.g., *Sibeck et al.*, 1987; *Zong et al.*, 2004, and references therein]. Significantly, the presence of such particles poorly correlates with conditions thought to generate boundary-normal magnetic fields (B_n) through magnetic reconnection. While specific instances of streaming particle distributions have been attributed to the presence of boundary-normal fields [e.g., *Paschmann et al.*, 1979; *Sonnerup et al.*, 1981; *Scholer et al.*, 1981, 1982], the mechanisms of energetic particle escape for general conditions and the role of reconnection and the associated B_n have not been determined.

The magnetic topology at the magnetopause as reflected in distributions of lower energy particles (eV to several keV) and magnetic fields is well documented [e.g., *Fuselier et al.*, 1995, 1997; *Lee et al.*, 2014] and is understood in terms of the characteristics of the low-latitude boundary layer (LLBL) [e.g., *Eastman et al.*, 1976] and the particles flowing on reconnected magnetic field lines just outside the magnetopause that constitute the magnetosheath boundary layer (MSBL) [e.g., *Cowley*, 1982]. For energetic particles, the most common signature attributed to the presence of finite B_n is monohemispheric streaming of energetic protons [*West and Buck*, 1976; *Eccles and Fritz*, 2002], sometimes associated with boundary-trapped energetic electrons [*Williams et al.*, 1979; *Scholer et al.*, 1982; *Daly*, 1982]. Observations of such streaming simultaneously in both energetic electrons and protons have been reported at the nightside flanks [*Mitchell et al.*, 1987; *Ogasawara et al.*, 2011], during strong compression in the dayside-dawn quadrant [*Korth et al.*, 1982], and for one more nominal

period in the near-nose prenoon regions [*Daly and Keppler*, 1982]. The unexpected dayside-dawn quadrant observations of simultaneous electron-proton streaming in the magnetosheath have not been previously reported.

The prevalence of energetic particle escape suggests that field-aligned transit along open magnetic fields is only one possible mechanism by which energetic magnetospheric particles cross the magnetopause. For example, it was proposed by *Sibeck et al.* [1987] that leakage mechanisms exist that do not require boundary-normal fields and that finite-gyroradius effects and scattering during such leakage can engender observed pitch angle streaming. Modeling of energetic particle transport across the magnetopause supports this claim, showing that guiding center gradient drift and finite-gyroradius scattering can also lead to escape and streaming [*Mauk et al.*, 2016]. New observations and/or techniques are needed to distinguish between different processes.

The observational advances afforded by the Magnetospheric Multiscale (MMS) mission [*Burch et al.*, 2015] allow us to address outstanding fundamental questions regarding energetic particle transport across the magnetopause. MMS comprises four spacecraft flying in formation with spacing (10–40 km) designed to address electron diffusion scales physics. For the mesoscale energetic particle phenomena addressed in the present paper, the measurements from the four spacecraft are largely indistinguishable. However, here we have made substantial use of magnetic field measurements from the four spacecraft to determine the thicknesses of the magnetopause boundaries, a critical parameter for the analysis of energetic particle escape. Other capabilities utilized here are the simultaneous ion and electron observations, ion compositional discrimination, pitch angle coverage, and sampling cadence of Energetic Ion Spectrometer (EIS) data. These allow us to address the following: What are the mechanisms of escape for energetic particles under various conditions? To what extent are boundary-normal magnetic fields required?

This report focuses on the simultaneous observation of multiple species (electrons, H^+, He^{n+}) in the dayside-dusk quadrant magnetosheath. While reporting here that such observations are common, we focus our attention on a repeatedly but less commonly observed signature featuring monohemispheric streaming in the LLBL (magnetospheric side) with a hemispheric depletion of field-aligned particles of near-0° (180°) that evolves into a streaming signature in the MSBL (magnetosheath side), with particle distributions strongly favoring >90° (<90°) pitch angles. The asymmetry relative to the magnetic field direction of these distributions on both sides of the magnetopause along with the large difference between the gyroradii of electrons and protons indicates that this loss unambiguously requires open field lines reconnected across the magnetopause boundary. Such a complete magnetosphere side/magnetosheath side signature simultaneously for electrons and ions has only previously been reported clearly by *Korth et al.* [1982] during an extreme compression event on the duskside. Similar features have been observed by others in ions [e.g., *Daly and Keppler*, 1982; *Eccles and Fritz*, 2002]; however, it is really only with the electrons that one can exclude finite gyroradius influences discussed by *Sibeck et al.* [1987]. While this phenomenon is generally unanticipated on the duskside because of the drift-shadowing of energetic electrons near the subsolar point, new EIS observations clearly show this feature at nominal distances of the dusk dayside magnetopause.

2. Observations and Analysis

Part of the Energetic Particle Detector (EPD) investigation on MMS, EIS measures energetic ion energy, angle, and compositional distributions from ~20 keV (protons), ~60 keV (helium), and ~130 keV (oxygen) up to ~1 MeV [*Mauk et al.*, 2014]. EIS also measures energetic electrons from 25 to 600 keV in support of the faster and more sensitive electron measurements made by the EPD Fly's Eye Energetic Particle Spectrometer (FEEPS) sensors [*Blake et al.*, 2015]. In the survey mode utilized here, EIS samples at 1/8 the spacecraft spin rate (~2.5 s). EIS adds two new elements to prior observations of energetic particle measurements at the magnetopause: measurement of ion elemental composition and its multiple (six) simultaneous views sample a complete angular distribution in one spin (~20 s).

Observations from the early MMS science phase (in the dayside dusk sector from about 13:00 to 18:00 LT) have shown that simultaneous monohemispheric streaming of both energetic electrons and light ions in the magnetosheath adjacent to the magnetopause occurs for ~50% of the magnetosheath excursions. Crossings that also exhibit anisotropic depletion in the LLBL (magnetospheric side) are less common. Seven such examples were found during September and October 2015. Here we present two cases that illustrate this pitch

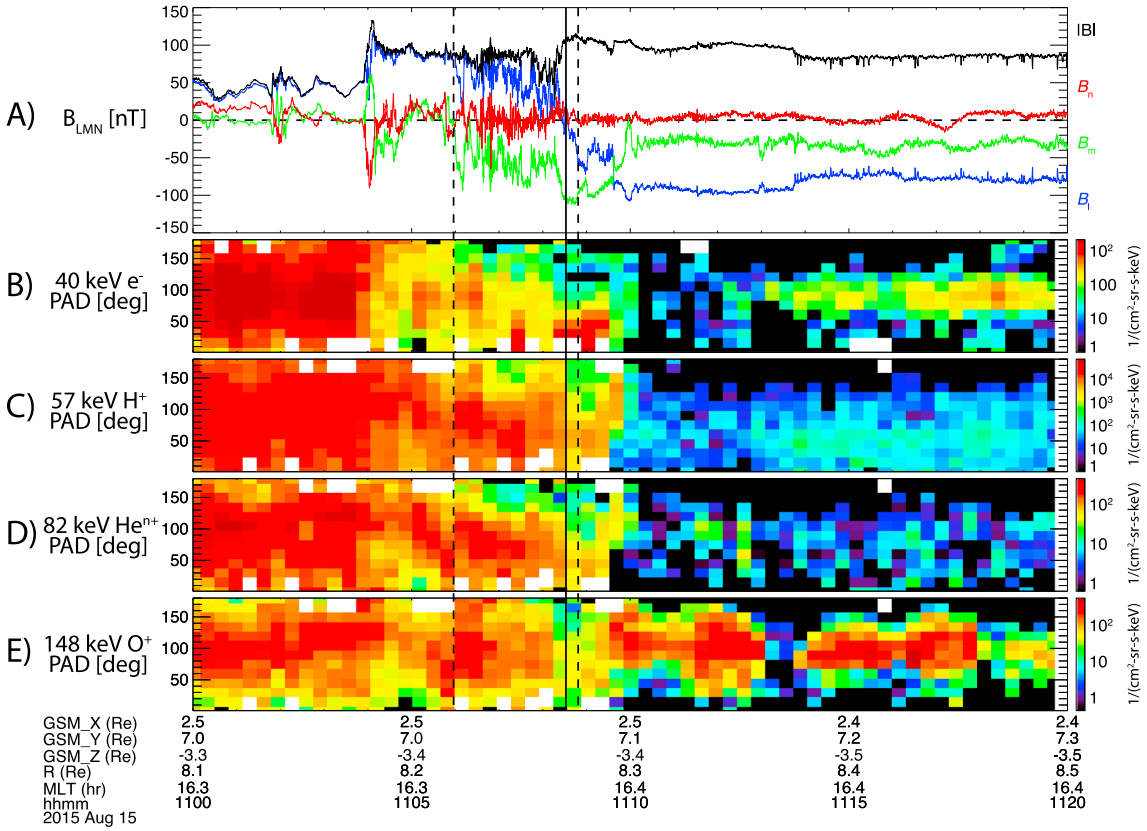

Figure 1. Magnetic field and energetic particle measurements from MMS2 during a 15 August 2015 magnetopause crossing. From the top, (first panel) magnetic field measurements from the MMS fluxgate magnetometer transformed into LMN coordinates using a magnetopause normal vector in the GSE coordinate system ($\hat{\mathbf{n}}_{MP}$) of (0.672386, 0.518808, −0.527955); black indicates the total field (B) and the components B_l (northward), B_m (dawnward), B_n ($MP_\perp$) are represented by blue, green, and red, respectively. The remaining panels show EIS observations of the pitch angle distributions for (second panel) 30–53 keV electrons, (third panel) 46–68 keV protons, (fourth panel) 60–110 keV helium ions, and (fifth panel) 130–170 keV oxygen ions. The vertical dashed lines identify the north-south component of the first and last encounters with the turbulent current layer, while the solid line indicates the time of the $B_l = 0$ point during the crossing. It should be noted that the magnetic field data for this event are from the commissioning phase of the mission. These data are prelevel two calibration and as such discrepancies up to a few tenths of a nanotesla, primarily in the spin axis component of the field, may remain and are not determined.

angle anisotropy transition, both of which occur during conditions of strong magnetopause erosion indicating strong dayside magnetic reconnection [*Anderson et al.*, 2016].

2.1. Case 1: 15 August 2015

Figure 1 shows an MMS3 magnetopause crossing from 15 August 2015. Figure 1a shows the magnetic field from the MMS fluxgate magnetometer (FGM) [*Torbert et al.*, 2014; *Russell et al.*, 2014] transformed into LMN coordinates using a magnetopause normal vector in GSE coordinates determined via minimum variance analysis of the magnetic field (MVAB) [cf. *Sonnerup and Scheible*, 1998]. The region prior to the current layer from 11:04 to 11:08 UT is identified as the LLBL.

Several features in Figures 1b to 1e of EIS particle data are of interest. First, the light ions (protons and helium) exhibit similar behavior, while oxygen demonstrates distinct dynamics that we attribute to its larger gyroradii. The charge state of the helium ions is unmeasured but is believed to be primarily He^{2+} with a smaller contribution of He^{+}. Differences between light ions and oxygen are common in the early EIS observations. The intensity of electrons decreases suddenly as the spacecraft enters the LLBL (11:04 UT), while the ion count rates do not decrease as much. This difference between electron and ion signatures of the LLBL may be due to the relatively larger ion gyroradii, which reduce the sensitivity of the ions to the variability in the field and/or changes in the field topology at the inner edge of the LLBL. For this crossing with a ~115 nT magnetosheath field and a particle energy of 50 keV, electrons, H^{+}, and O^{+} have gyroradii of 6.4, 280, and 1120 km, respectively. The average magnetopause thickness for this crossing is ~500 km (cf. section 3). A second feature of interest is the general decrease in the electron and light ion intensities for pitch angles close to 180° as the

spacecraft approaches the center of the current sheet where $B_l \approx 0$ (11:06 to 11:08 UT), with some excursions from the trend associated with magnetic variability. On the magnetosheath side of the current layer, from 11:08:20 to 11:09:40 UT, both electrons and protons are monohemispheric, confined to pitch angles <90°. We interpret this region as the MSBL. The field has completed the majority of its rotation from magnetospheric to magnetosheath orientation by 11:08:20 UT. There is a transition from <90° to >90° pitch angles in the proton data at approximately 11:09:30 UT at the end of the MSBL. This transition is correlated with a magnetic field discontinuity and is perhaps the light ions' pitch angle response to the field rotation [cf. *Sibeck et al.*, 1987].

As discussed in section 3, we interpret the loss of >90° pitch angles in the LLBL (magnetospheric side) and the transition to primarily <90° distributions in the MSBL (magnetospheric side) as a consequence of particle escape in the presence of a finite B_n at the magnetopause. The depletion of near 180° pitch angles in the LLBL requires a finite B_n. In agreement with prior observations from other dayside regions [*Korth et al.*, 1982; *Daly and Keppler*, 1982] we hypothesize that the spacecraft transitions from field lines that are not connected to the magnetopause (yielding symmetric pitch angle distributions), to field lines on the magnetosphere side that are connected to the magnetopause (yielding asymmetric pitch angle distributions due to the absence of a source of energetic particles at the magnetopause), and finally to magnetopause-connected field lines in the magnetosheath (with pitch angle distributions that are streaming anti-Earthward; cf. Figure 3f). Because of their small gyroradii, it is the simultaneous electron features (also seen by *Korth et al.* [1982]) that offer the most compelling evidence for this interpretation.

2.2. Case 2: 7 September 2015

Figures 2a–2g show FGM and EIS data from MMS2 for a 6 h period (12:00 to 18:00 UT) encompassing multiple magnetopause crossings on 7 September 2015. Figure 2a shows our identification of the magnetosphere, boundary layer (either LLBL or MSBL), and magnetosheath regions. This period exemplifies the complexity of energetic particle dynamics at the magnetopause. As indicated in Figure 2a, MMS2 is initially in the energetic particle-rich magnetosphere, measuring relatively constant particle intensities. It then enters a transitional region (first green region in Figure 2a) characterized by significant variability in the magnetic field and mixing of the $\lesssim$15 keV protons (of assumed magnetosheath origin; Figure 2e) and more energetic ~15 to ~30 keV magnetospheric protons. Here we do not distinguish between LLBL and MSBL. The boundary layer is again marked by a noticeable drop in the energetic electron signatures relative to the protons as in Case 1. The spacecraft then makes a brief excursion into the magnetosheath where it observes only $\lesssim$15 keV protons and increased magnetic field magnitude (relative to the magnetosphere). There are several more transitions through these three regions until a sharp magnetopause crossing at approximately 14:22 UT that brings the spacecraft into the magnetosheath for an extended duration. The abrupt southward turning of the magnetic field indicates the magnetopause current layer for the crossing at 14:22 UT.

The magnetosheath interval exhibits varied energetic particle dynamics with multiple enhancements in energetic protons and oxygen. Initial analysis of EIS data indicates that enhancements of magnetospheric ions of comparable intensities outside the magnetopause are fairly common, as expected [e.g., *Peterson et al.*, 1982; *Fuselier et al.*, 1991; *Chen and Fritz*, 1999]. The substantial increase of energetic particles of all species seen from approximately 15:30 to 16:02 UT and the increase of oxygen relative to that inside the magnetosphere are likely results of injected and accelerated energetic particles from the magnetotail that have drifted to and either reached (with large gyroradii) or been transported across the magnetopause. A similar O^+ enhancement event is studied by J.H. Westlake et al. (The Permeability of the Magnetopause to a Multispecies Substorm Injection of Energetic Particles, submitted to *Geophysical Research Letters*, 2016).

Of primary interest here is the sharp magnetopause crossing at approximately 14:22 UT. Figures 2h–2q show an expanded view of this region with additional parameters provided by the Dual Ion Spectrometer (DIS) instrument, part of the Fast Plasma Investigation (FPI) [*Pollock et al.*, 2016], and burst resolution electron pitch angles from the FEEPS instrument. The vertical black line indicates the approximate center of the magnetopause crossing characterized by a rotation in the B_l component of the magnetic field (the field magnitude monotonically increases) and a transition to colder, denser plasma. The plasma flow velocities transition from slower flows in the magnetosphere to stronger magnetosheath flows. The southward excursion of the flow (red curve in Figure 2k) for 1 min prior to the magnetopause crossing is of particular significance. The intervals from 14:20 to 14:21:30 UT and 14:21:30 to 14:22:20 UT (marked by dashed lines) are identified as LLBL and MSBL, respectively.

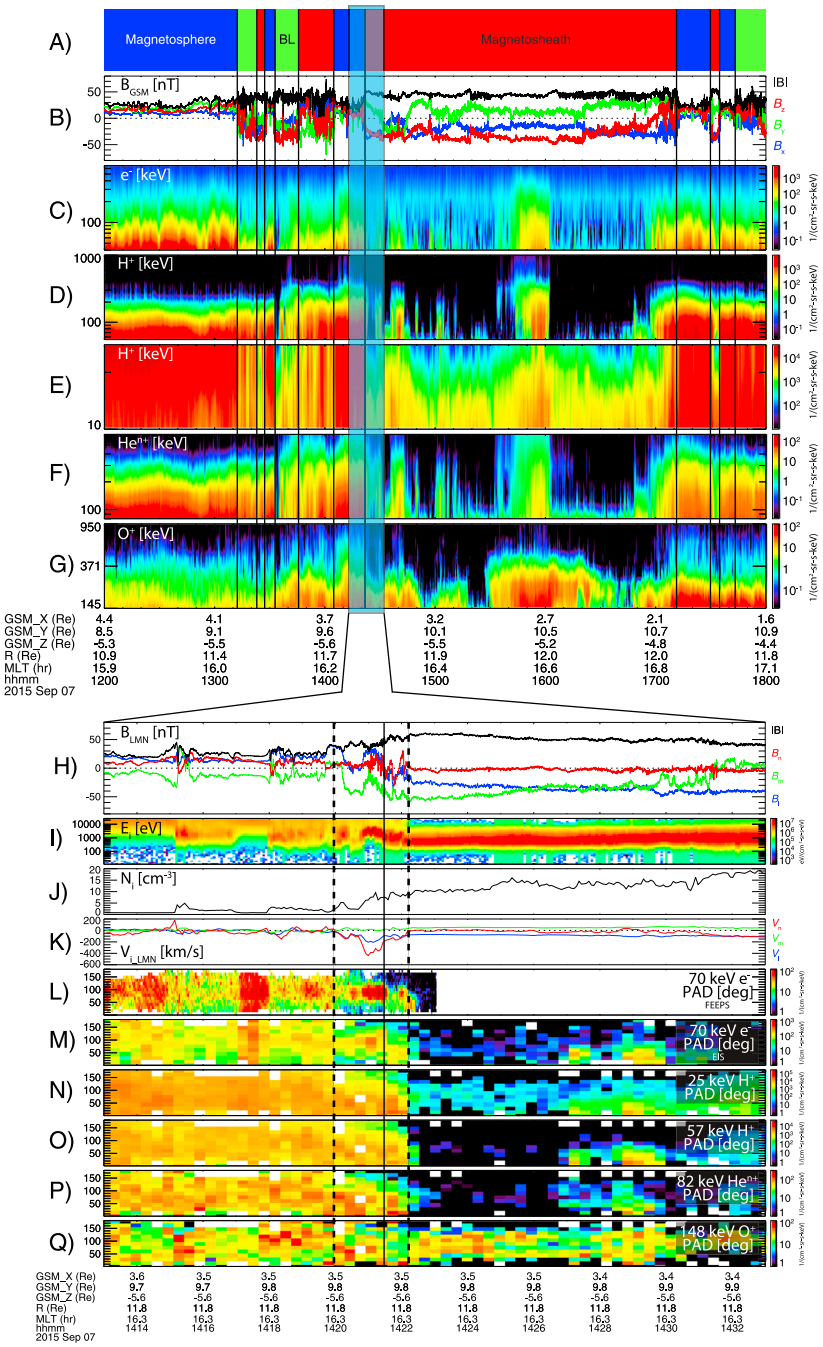

Figure 2. Six hour period encompassing multiple complete and partial crossings of the magnetopause by the MMS2 spacecraft from 12:00 to 18:00 UT on 7 September 2015. (a) Our identification of the different topological regions traversed by the spacecraft (magnetosphere in blue, a broadly termed "boundary layer" of mixed magnetospheric and magnetosheath plasma in green, and magnetosphere in red). (b) Magnetic field measurements in GSM coordinates: B (black), B_x (blue), B_y (green), B_z (red). Energy spectrograms for (c) electrons, (d, e) protons (two energy ranges), (f) helium, and (g) oxygen from EIS. Figures 2h–2q focus on the final sharp magnetopause crossing at approximately 14:22 UT on 7 September 2015 showing additional parameters than those presented in Figures 2a–2g. The vertical lines identify the north-south component of first and last encounters with the turbulent current layer (dashed) and the time of the $B_l = 0$ point during the crossing (solid). (h) The magnetic field in LMN coordinates using an MVAB-calculated $\hat{\mathbf{n}}_{MP}$ of (0.638731, 0.436986, −0.633297). (I) The ion energy spectrum from the Dual Ion Spectrometer (DIS) instrument, part of the Fast Plasma Investigation (FPI). The (j) ion density and (k) bulk velocity (in LMN coordinates), from DIS. (l) FEEPS burst and (m) EIS survey resolution of pitch angle distributions for 54–90 keV electrons. EIS pitch angle distributions for (n) 46–68 keV protons, (o) 20–30 keV protons, (p) 60–111 keV helium, and (q) 129–169 keV oxygen from EIS.

The energetic particle pitch angle distributions resemble those identified for Case 1. Electrons, protons, and the helium ions transition from having roughly symmetric pitch angle distributions (prior to 14:20 UT), to asymmetric pitch angle distributions in the LLBL with the lowest intensities close to 180° (between ~14:20 and 14:21:30), and then to monohemispheric distributions outside of the magnetopause in the MSBL with distributions confined primarily to the <90° regime (beyond 14:21:30 UT). As interpreted for Case 1, we infer that this sequence of distributions is due to the presence of a finite B_n; this is supported here by the nonzero B_n component calculated via MVAB analysis (Figure 2h). Further asymmetric pitch angles in the magnetosheath from approximately 14:27 to 14:30 UT indicate additional escape from a remote location along the magnetopause, implying that escaping particles are not necessarily encountering the magnetopause at a position local to the spacecraft. As in Case 1, the behavior of energetic oxygen ions is different from the lighter ions.

Several observations support our interpretation that the energetic particle signature of asymmetric depletion in the LLBL transitioning to monohemispheric streaming in the MSBL is associated with a finite B_n created by magnetic reconnection. First, the plasma and magnetic field data show classic signatures associated with reconnection and boundary-normal magnetic fields [cf. *Scholer et al.*, 1981]. Second, for this event, the interplanetary magnetic field (IMF) (not shown) was directed southward and slightly duskward corresponding to a reconnection line north of the magnetic equator and MMS, as supported by the predicted location of the reconnection line [*Trattner et al.*, 2007a, 2007b; *Fuselier et al.*, 2014] and its relationship to the MMS location shown in Figure S1 in the supporting information. Finally, Active Magnetosphere and Planetary Electrodynamics Response Experiment (AMPERE) field-aligned currents (not shown) further support this conclusion implying a positive IMF B_y.

3. Discussion

The evolution of the energetic particle pitch angle distributions during the two events presented here motivated the single-particle trajectory model for the interactions of energetic particles with an idealized magnetopause structure documented in a companion paper by *Mauk et al.* [2016]. This model generalizes prior models in several ways that emulate the rotational structures within the magnetopause boundary: (1) the magnetic gradients on the magnetosphere side and magnetosheath side are independent; (2) it allows arbitrary magnetic field rotations at the magnetopause; (3) it incorporates gradients associated with draping field lines on the magnetosheath side and electric fields associated with fast flows in the magnetosheath; and (4) it allows for a finite B_n as a fraction of the total magnetosheath field. The model supports the conclusions of *Sibeck et al.* [1987], showing that electrons and protons can escape in different ways depending on the magnetopause configuration: e.g., drift across the boundary (either in a guiding center sense or via finite gyroradius effects) even in the absence of a boundary-normal field and escape along boundary-normal fields with substantial modifications arising from large gyroradius effects. Figure 3 shows results from this model obtained by injecting a specified angular distribution of particles on the magnetosphere side and tracking their interactions with the magnetopause to generate simulated pitch angle distributions for comparison with the EIS observations.

The parameters used in the model were derived from the magnetopause crossing of Case 2. In addition to the observed magnetic field and plasma flows, the model also requires a magnetopause thickness (d_{MP}). To estimate this, we used FGM and ephemeris data from all four MMS observatories and considered three distinct current sheet crossings: 14:19:54 – 14:20:43 UT, 14:20:37 – 14:21:10 UT, and 14:21:03 – 14:22:26 UT. For each crossing, we determined the magnetopause normal ($\hat{\mathbf{n}}_{MP}$) from both the average of the minimum variance of **B** at each observatory and the minimum variance of the current density, (**J**), derived from the discrete curl of **B** across all four spacecraft. We then fit the B_l profile in time to a Fermi function written as

$$f(t, t_0, a, b, \delta) = \frac{a}{\left(1 + e^{\frac{-(t-t_0)}{\delta}}\right)} + b, \tag{1}$$

where b is the initial value, a is the change, t_0 gives the center time of the crossing, and 4δ is the transit time. The latter follows since the slope of f at $t = t_0$ times 4δ gives the change, a. This analysis provides both a center time and a transit time for each crossing at each spacecraft. Denoting the center time of the crossing at the ith spacecraft as t_{0i} and the position of the ith spacecraft as $\mathbf{r}_i$, the time difference ($dt_{ij} = t_{0j} - t_{0i}$), position difference ($d\mathbf{r}_{ij} = \mathbf{r}_j - \mathbf{r}_i$), and separation ($dr_{ij} = |d\mathbf{r}_{ij}|$), are related to an assumed constant velocity of the boundary (**V**) by

$$dt_{ij}(\hat{\mathbf{n}}_{ij} \cdot \mathbf{V}) = dr_{ij}, \tag{2}$$

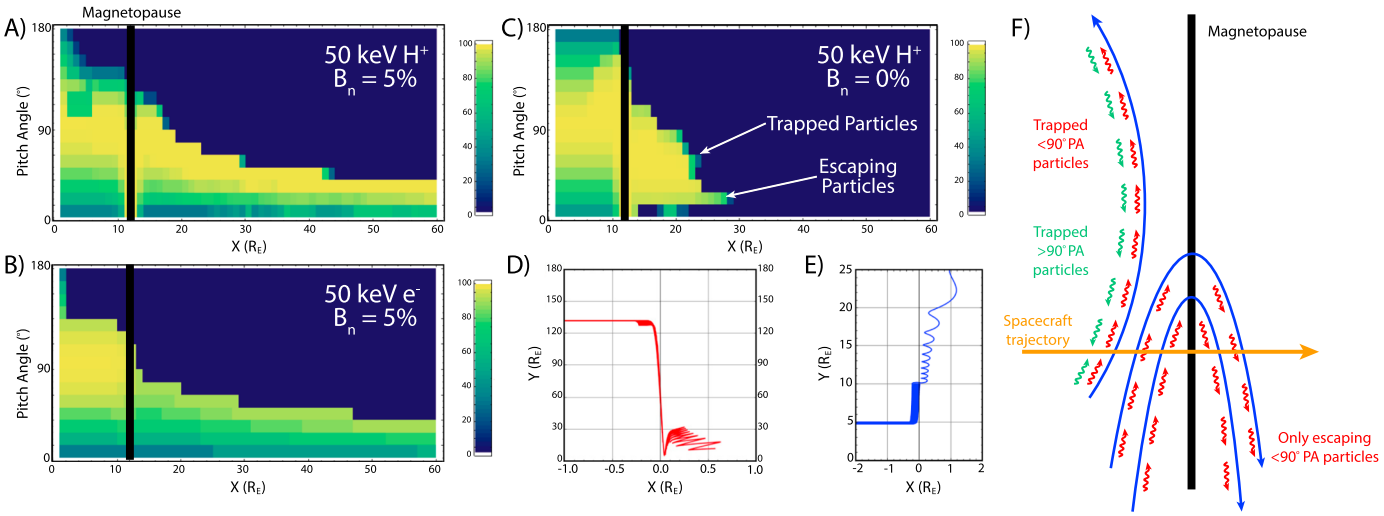

Figure 3. Simulated pitch angle displays based on *Mauk et al.* [2016] model generated by injecting a specified angular distribution of particles on the magnetospheric side and tracking their interactions with the modeled magnetopause. The runs shown here use parameters derived from the magnetopause crossing shown in Figure 2 as discussed in the text. Simulated pitch angle distributions for a (a) 50 keV proton and (b) 50 keV electron, crossing a 600 km thick magnetopause (black line) for cases with a B_n component that is 5% of the total magnetosheath field strength. (c) This demonstrates that even instances without a normal component of the magnetic field can still result in the escape of field-aligned particles that orbit along the magnetopause boundary and escape farther downtail. These characteristics are demonstrated in Figures 3d and 3e, showing respectively, (d) the pitch angle evolution of a single 50 keV proton from the case shown in Figure 3c and (e) its trajectory escaping across the magnetopause (in model-defined coordinates). Note that this simple model has magnetospheric magnetic gradients coplanar to the magnetopause. (f) A schematic of the spacecraft's closed-to-open field line transition of the spacecraft that explains the complete novel asymmetric pitch angle signatures reported here.

where $\hat{\mathbf{n}}_{ij} = d\mathbf{r}_{ij}/dr_{ij}$. This overdetermined linear equation was solved for $\mathbf{V}$ using singular value decomposition. The thickness of the boundary was derived by projecting the displacement ($\mathbf{V}dt$) along the normal to the magnetopause ($\hat{\mathbf{n}}_{MP}$), to give $d_{MP} = dt(\hat{\mathbf{n}}_{MP} \cdot \mathbf{V})$, where dt is the average of dt_{ij}. For these three crossings this analysis yields an average thickness of 600 km with a minimum of 300 km, maximum of 1070 km, and a standard deviation of 275 km.

Model results, using the average thickness and other observed quantities, are shown in Figure 3. For $B_n \neq 0$ (Figures 3a and 3b), the pitch angle patterns for the magnetosphere-to-magnetosheath transition are quite similar to those observed for Cases 1 and 2, showing asymmetric pitch angle depletion in the LLBL with a transition to monohemispheric streaming in the MSBL. However, observation of monohemispheric streaming alone is not enough to imply the presence of a B_n component. Figure 3c demonstrates such a case without a B_n component. Here many protons entrained along the boundary reach out into the magnetosheath due to finite gyroradius effects (as shown by *Daly* [1982]), while others escape due to the field rotation or scattering effects [*Mauk et al.*, 2016] and produce a monohemispheric streaming signature in the sheath. Figures 3d and 3e show the trajectory and pitch angle evolution for one such particle. Figure 3c shows a finite gyroradius engendered pitch angle anisotropy on the magnetospheric side, but the sense of that anisotropy is the opposite of the observed streaming on the magnetosheath side. Thus, it is the complete signature reported here, with the asymmetric pitch angle depletion in both the LLBL and MSBL, that provides evidence for the presence of a B_n component as the spacecraft transitions from closed terrestrial magnetic field lines in the magnetosphere to reconnected field lines that are open across the boundary (Figure 3f).

The model reveals that particles can move substantial distances along the magnetopause [i.e., *Speiser et al.*, 1981; *Speiser and Williams*, 1982] before they escape. Electrons can escape at different positions than protons, and the escaping particles are likely to be observed in a spatially structured way, as observed from 14:27 to 14:33 UT in Figure 2. It is unclear how energetic electrons can so commonly gain access to the dusk-dayside quadrant of the magnetopause for escape given that this region is magnetically drift-shadowed. The escaping electrons in the LLBL (magnetospheric side) are observed over extended periods of time (minute time scales) and given that they should escape almost instantaneously (greater than seconds) once on an open field line on the time scale studied here, a continuous source of electrons is needed inside the magnetosphere [*Scholer et al.*, 1981; *Korth et al.*, 1982]. Within a few R_E of the magnetopause, the gradient of the magnetic

field may approach zero resulting in electron gradient drift speeds significantly lower than typically observed flow speeds. It is therefore possible that the electron dynamics in this region is flow dominated and the static picture of magnetopause shadowing of electrons from the afternoon outer magnetosphere is an oversimplification. Electrons need to be transported from unconnected field lines onto open reconnected magnetic field lines in a roughly continuous fashion, perhaps through a combination of erosion (the continuous opening up of new field lines) and some combination of magnetic and electric drifts roughly parallel to the magnetopause.

4. Conclusion

Initial results from the MMS/EIS instrument commonly show energetic particles (greater than tens of keV) in the dayside-dusk quadrant magnetosheath near the magnetopause that are likely of magnetospheric origin. These represent the first reported dayside dusk observations of simultaneous monohemispheric streaming in both electrons and light ions in the magnetosheath at nominal magnetopause distances. The regular observation of this feature is unexpected because the duskside regions are expected to be magnetic drift-shadowed from electrons. Sparse previous reports of such simultaneous streaming on the dayside have been limited to dawn and prenoon regions [*Korth et al.*, 1982; *Daly and Keppler*, 1982].

The present study focused on a particular class of simultaneous electron/ion streaming in the magnetosheath, namely, those which exhibit loss of field-aligned pitch angles for both light ions and electrons on the magnetospheric side of the current layer (LLBL) together with depletion of the same field-aligned pitch angle populations of both light ions and electrons on the magnetosheath side of the boundary (MSBL). For reconnection northward of the satellite, the depleted pitch angles are near 180° such that particles with <90° remain, as observed in the two cases presented here. For reconnection south of the spacecraft, pitch angles >90° would be preferentially lost. The observations of monohemispheric streaming in the MSBL (magnetosheath side) do not necessarily require a finite B_n at the magnetopause (also shown by *Sibeck et al.* [1987] and *Mauk et al.* [2016]). However, our observations of simultaneous electron and ion streaming associated with depletion in the LLBL (magnetospheric side) do require a normal component of the magnetopause magnetic field. The results of these case analyses indicate how the simultaneous high cadence, broad pitch angle coverage, and species discrimination capabilities of the EPD instrumentation can offer new insight into the dynamics of energetic particles at the magnetopause.

Acknowledgments
The authors are grateful to the dedicated scientists and engineers of the MMS science, instrument, and operations teams. The Magnetospheric Multiscale (MMS) mission is funded under NASA contract NNG04EB99C. As of 1 March 2016, MMS data are available for 1 September 2015 through 31 January 2016 from the MMS Science Data Center website: https://lasp.colorado.edu/mms/sdc/. Data for 15 August 2015 are available upon request.

References

Anderson, B. J., et al. (2016), Electrodynamic context of magnetopause dynamics observed by magnetospheric multiscale, *Geophys. Res. Lett.*, *43*, doi:10.1002/2016GL069577.

Blake, J. B., et al. (2015), The fly's eye energetic particle spectrometer (FEEPS) sensors for the magnetospheric multiscale (MMS) mission, *Space Sci. Rev.*, *199*(1), 309–329, doi:10.1007/s11214-015-0163-x.

Burch, J. L., T. E. Moore, R. B. Torbert, and B. L. Giles (2015), Magnetospheric multiscale overview and science objectives, *Space Sci. Rev.*, 1–17, doi:10.1007/s11214-015-0164-9.

Chen, J., and T. A. Fritz (1999), May 4, 1998 storm: Observations of energetic ion composition by POLAR, *Geophys. Res. Lett.*, *26*(19), 2921–2924, doi:10.1029/1999GL003582.

Cowley, S. W. H. (1982), The causes of convection in the Earth's magnetosphere: A review of developments during the IMS, *Rev. Geophys.*, *20*(3), 531–565, doi:10.1029/RG020i003p00531.

Daly, P. W. (1982), Remote sensing of energetic particle boundaries, *Geophys. Res. Lett.*, *9*(12), 1329–1332, doi:10.1029/GL009i012p01329.

Daly, P. W., and E. Keppler (1982), Observation of a flux transfer event on the earthward side of the magnetopause, *Planet. Space Sci.*, *30*(4), 331–337, doi:10.1016/0032-0633(82)90038-1.

Eastman, T. E., E. W. Hones, S. J. Bame, and J. R. Ashbridge (1976), The magnetospheric boundary layer: Site of plasma, momentum and energy transfer from the magnetosheath into the magnetosphere, *Geophys. Res. Lett.*, *3*(11), 685–688, doi:10.1029/GL003i011p00685.

Eccles, A. A., and T. A. Fritz (2002), Energetic particle observations at the subsolar magnetopause, *Ann. Geophys.*, *20*(4), 445–460, doi:10.5194/angeo-20-445-2002.

Fuselier, S. A., D. M. Klumpar, and E. G. Shelley (1991), On the origins of energetic ions in the Earth's dayside magnetosheath, *J. Geophys. Res.*, *96*(A1), 47–56, doi:10.1029/90JA01751.

Fuselier, S. A., B. J. Anderson, and T. G. Onsager (1995), Particle signatures of magnetic topology at the magnetopause: AMPTE/CCE observations, *J. Geophys. Res.*, *100*(A7), 11,805–11,821, doi:10.1029/94JA02811.

Fuselier, S. A., B. J. Anderson, and T. G. Onsager (1997), Electron and ion signatures of field line topology at the low-shear magnetopause, *J. Geophys. Res.*, *102*(A3), 4847–4863, doi:10.1029/96JA03635.

Fuselier, S. A., W. S. Lewis, C. Schiff, R. E. Ergun, J. L. Burch, S. M. Petrinec, and K. J. Trattner (2014), Magnetospheric multiscale science mission profile and operations, *Space Sci. Rev.*, *199*(1), 77–103, doi:10.1007/s11214-014-0087-x.

Korth, A., G. Kremser, P. W. Daly, and E. Amata (1982), Observations of field-aligned energetic electron and ion distributions near the magnetopause at geosynchronous orbit, *J. Geophys. Res.*, *87*(A12), 10,413–10,419, doi:10.1029/JA087iA12p10413.

Lee, S. H., H. Zhang, Q.-G. Zong, A. Otto, D. G. Sibeck, Y. Wang, K.-H. Glassmeier, P. W. Daly, and H. Rème (2014), Plasma and energetic particle behaviors during asymmetric magnetic reconnection at the magnetopause, *J. Geophys. Res. Space Physics*, *119*(3), 1658–1672, doi:10.1002/2013JA019168.

Mauk, B. H., et al. (2014), The energetic Particle Detector (EPD) investigation and the Energetic Ion Spectrometer (EIS) for the Magnetospheric Multiscale (MMS) mission, *Space Sci. Rev.*, *199*(1), 471–514, doi:10.1007/s11214-014-0055-5.

Mauk, B. H., I. J. Cohen, J. H. Westlake, and B. J. Anderson (2016), Modeling magnetospheric energetic particle escape across Earth's magnetopause as observed by the MMS mission, *Geophys. Res. Lett.*, *43*, 4081–4088, doi:10.1002/2016GL068856.

Mitchell, D. G., F. Kutchko, D. J. Williams, T. E. Eastman, L. A. Frank, and C. T. Russell (1987), An extended study of the low-latitude boundary layer on the dawn and dusk flanks of the magnetosphere, *J. Geophys. Res.*, *92*(A7), 7394–7404, doi:10.1029/JA092iA07p07394.

Ogasawara, K., S. A. Livi, D. G. Mitchell, T. P. Armstrong, and N. Krupp (2011), Properties of energetic particle bursts at dawnside magnetosheath: Cassini observations during the 1999 Earth swing-by, *J. Geophys. Res.*, *116*, A12207, doi:10.1029/2011JA016813.

Paschmann, G., B. U. Ö. Sonnerup, I. Papamastorakis, N. Sckopke, G. Haerendel, S. J. Bame, J. R. Ashbridge, J. T. Gosling, C. T. Russell, and R. C. Elphic (1979), Plasma acceleration at the Earth's magnetopause: Evidence for reconnection, *Nature*, *282*(5736), 243–246, doi:10.1038/282243a0.

Peterson, W. K., E. G. Shelley, G. Haerendel, and G. Paschmann (1982), Energetic ion composition in the subsolar magnetopause and boundary layer, *J. Geophys. Res.*, *87*(A4), 2139–2145, doi:10.1029/JA087iA04p02139.

Pollock, C. J., et al. (2016), Fast plasma investigation for magnetospheric multiscale, *Space Sci. Rev.*, *199*(1), 331–406, doi:10.1007/s11214-016-0245-4.

Russell, C. T., et al. (2014), The magnetospheric multiscale magnetometers, *Space Sci. Rev.*, *199*(1), 189–256, doi:10.1007/s11214-014-0057-3.

Scholer, M., F. M. Ipavich, G. Gloeckler, D. Hovestadt, and B. Klecker (1981), Leakage of magnetospheric ions into the magnetosheath along reconnected field lines at the dayside magnetopause, *J. Geophys. Res.*, *86*(A3), 1299–1304, doi:10.1029/JA086iA03p01299.

Scholer, M., P. W. Daly, G. Paschmann, and T. A. Fritz (1982), Field line topology determined by energetic particles during a possible magnetopause reconnection event, *J. Geophys. Res.*, *87*(A8), 6073–6080, doi:10.1029/JA087iA08p06073.

Sibeck, D. G., R. W. McEntire, A. T. Y. Lui, R. E. Lopez, S. M. Krimigis, R. B. Decker, L. J. Zanetti, and T. A. Potemra (1987), Energetic magnetospheric ions at the dayside magnetopause: Leakage or merging?, *J. Geophys. Res.*, *92*(A11), 12,097–12,114, doi:10.1029/JA092iA11p12097.

Sonnerup, B. U. Ö., and M. Scheible (1998), Minimum and maximum variance analysis, in *Analysis Methods for Multi-Spacecraft Data*, edited by G. Paschmann and P. W. Daly, pp. 185–220, Int. Space Sci. Inst., Bern.

Sonnerup, B. U. Ö., G. Paschmann, I. Papamastorakis, N. Sckopke, G. Haerendel, S. J. Bame, J. R. Ashbridge, J. T. Gosling, and C. T. Russell (1981), Evidence for magnetic field reconnection at the Earth's magnetopause, *J. Geophys. Res.*, *86*(A12), 10,049–10,067, doi:10.1029/JA086iA12p10049.

Speiser, T. W., and D. J. Williams (1982), Magnetopause modeling: Flux transfer events and magnetosheath quasi-trapped distributions, *J. Geophys. Res.*, *87*(A4), 2177–2186, doi:10.1029/JA087iA04p02177.

Speiser, T. W., D. J. Williams, and H. A. Garcia (1981), Magnetospherically trapped ions as a source of magnetosheath energetic ions, *J. Geophys. Res.*, *86*(A2), 723–732, doi:10.1029/JA086iA02p00723.

Torbert, R. B., et al. (2014), The FIELDS instrument suite on MMS: Scientific objectives, measurements, and data products, *Space Sci. Rev.*, *199*(1), 105–135, doi:10.1007/s11214-014-0109-8.

Trattner, K. J., J. S. Mulcock, S. M. Petrinec, and S. A. Fuselier (2007a), Location of the reconnection line at the magnetopause during southward IMF conditions, *Geophys. Res. Lett.*, *34*, L03108, doi:10.1029/2006GL028397.

Trattner, K. J., J. S. Mulcock, S. M. Petrinec, and S. A. Fuselier (2007b), Probing the boundary between antiparallel and component reconnection during southward interplanetary magnetic field conditions, *J. Geophys. Res.*, *112*, A08210, doi:10.1029/2007JA012270.

West, H. I., and R. M. Buck (1976), Observations of >100-keV protons in the Earth's magnetosheath, *J. Geophys. Res.*, *81*(4), 569–584, doi:10.1029/JA081i004p00569.

Williams, D. J., T. A. Fritz, B. Wilken, and E. Keppler (1979), An energetic particle perspective of the magnetopause, *J. Geophys. Res.*, *84*(A11), 6385–6396, doi:10.1029/JA084iA11p06385.

Zong, Q.-G., T. A. Fritz, H. E. Spence, K. Oksavik, Z.-Y. Pu, A. Korth, and P. W. Daly (2004), Energetic particle sounding of the magnetopause: A contribution by Cluster/RAPID, *J. Geophys. Res.*, *109*(A04207), 1–14, doi:10.1029/2003JA009929.